Astronomical Journal, IN PRESS
Preprint typeset using LaTeX style AASTeX6 v. 1.0

arXiv:1704.00203v2 [astro-ph.EP] 21 Jun 2017

ABSENCE OF A METALLICITY EFFECT FOR ULTRA-SHORT-PERIOD PLANETS[1]

JOSHUA N. WINN[2], ROBERTO SANCHIS-OJEDA[3], LESLIE ROGERS[4], ERIK A. PETIGURA[5], ANDREW W. HOWARD[5], HOWARD ISAACSON[3], GEOFFREY W. MARCY[3], KEVIN C. SCHLAUFMAN[6], PHILLIP CARGILE[7], AND LESLIE HEBB[8]

[1]Based on observations obtained at the W. M. Keck Observatory, which is operated jointly by the University of California and the California Institute of Technology. Keck time was granted by NASA, the University of California, the California Institute of Technology, and the University of Hawaii.

[2]Department of Astrophysical Sciences, Princeton University, 4 Ivy Lane, Princeton, NJ 08540, USA
[3]Department of Astronomy, University of California, Berkeley, CA 94720
[4]Department of Astronomy & Astrophysics, University of Chicago, 5640 South Ellis Avenue, Chicago, IL 60637, USA
[5]Department of Astronomy, California Institute of Technology, Pasadena, CA 91125, USA
[6]Department of Physics and Astronomy, Johns Hopkins University, Baltimore, MD 21218, USA
[7]Harvard-Smithsonian Center for Astrophysics, 60 Garden St, Cambridge, MA 02138, USA
[8]Hobart and William Smith Colleges, Geneva, NY 14456, USA

ABSTRACT

Ultra-short-period (USP) planets are a newly recognized class of planets with periods shorter than one day and radii smaller than about 2 $R_\oplus$. It has been proposed that USP planets are the solid cores of hot Jupiters that lost their gaseous envelopes due to photo-evaporation or Roche lobe overflow. We test this hypothesis by asking whether USP planets are associated with metal-rich stars, as has long been observed for hot Jupiters. We find the metallicity distributions of USP-planet and hot-Jupiter hosts to be significantly different ($p = 3 \times 10^{-4}$), based on Keck spectroscopy of *Kepler* stars. Evidently, the sample of USP planets is not dominated by the evaporated cores of hot Jupiters. The metallicity distribution of stars with USP planets is indistinguishable from that of stars with short-period planets with sizes between 2–4 $R_\oplus$. Thus it remains possible that the USP planets are the solid cores of formerly gaseous planets smaller than Neptune.

Keywords: planetary systems—planets and satellites: detection, atmospheres

1. INTRODUCTION

The discovery of planets with orbital periods shorter than one day, and comparable in size to the Earth, has sparked discussion about their origin and evolution. The first well-documented planets in this category were CoRoT-7b (Léger et al. 2009), Kepler-10b (Batalha et al. 2011), 55 Cnc e (Dawson & Fabrycky 2010; Winn et al. 2011; Demory et al. 2011), and Kepler-78b (Sanchis-Ojeda et al. 2013). A sample of about 100 such planets was drawn together from *Kepler* data and analyzed by Sanchis-Ojeda et al. (2014). An independent *Kepler* survey was performed by (Jackson et al. 2013), and new examples have since been discovered by Becker et al. (2015), Adams et al. (2016), and Vanderburg et al. (2016).

Among the hypotheses for the origin of these "ultra-short-period" (USP) planets is that they are the exposed solid cores of hot Jupiters that formed through core accretion. As circumstantial evidence for a connection between USP planets and hot Jupiters, Sanchis-Ojeda et al. (2014) and Steffen & Coughlin (2016) noted that these two categories of planets are both found around ≈0.5% of FGK stars. They also found that USP planets are almost always smaller than 2 $R_\oplus$, putting them in or near the size range for which planets are thought to have a mainly rocky composition (Weiss & Marcy 2014; Rogers 2015). They hypothesized that the most strongly irradiated hot Jupiters eventually lose their gaseous envelopes due to photo-evaporation or Roche lobe overflow (Valsecchi et al. 2014). This would leave behind a nearly-naked core in a close-in orbit. Proving this hypothesis to be correct would confirm the core-accretion theory, and enable direct measurements of the size and mass distribution of the rocky cores that nucleate the growth of giant planets.

However, there are other possibilities for the origin of the USP planets. They might represent the short-period extension of the distribution of close-in rocky planets which either formed by core accretion in their current orbits (Chiang & Laughlin 2013), or migrated inwards from more distant orbits (Ida & Lin 2004; Schlaufman et al. 2010; Terquem 2014). Another possibility is that the USP planets are the exposed remnants not of hot Jupiters, but of smaller gaseous planets with sizes between 2-4 $R_\oplus$ (Lundkvist et al. 2016; Lee & Chiang 2017).

Here we test for a connection between USP planets and hot Jupiters by comparing the metallicities of their host stars. Stars that host giant planets with orbital periods shorter than

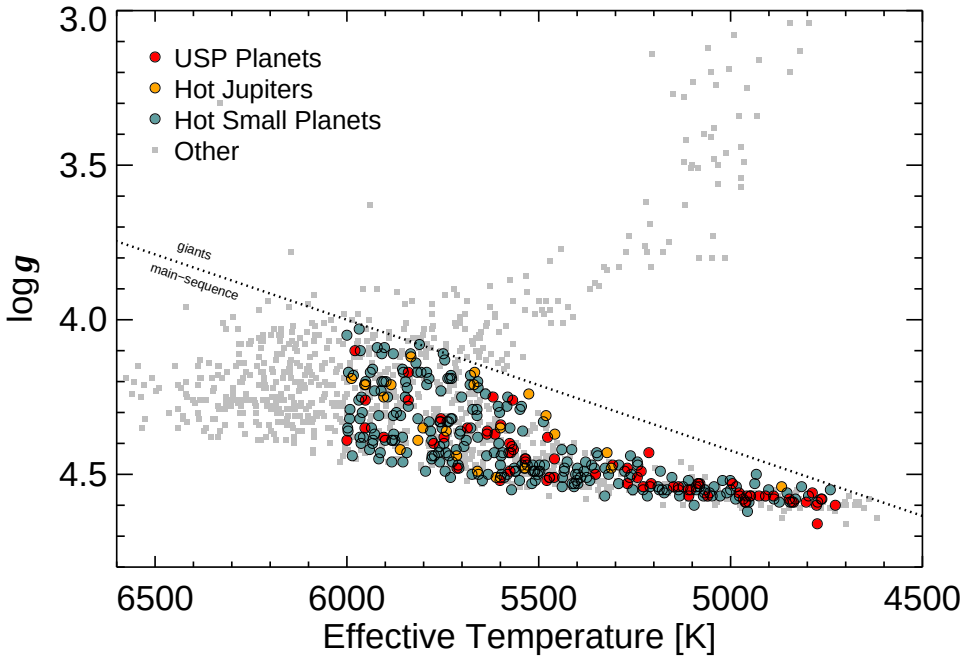


Figure 1. Spectroscopic parameters of the stellar samples. Stars below the dashed line were deemed main-sequence stars for the purpose of constructing our statistical samples, as described in §3. Colored circles show the parameters of the sample stars. The smaller squares are the broader sample of stars in the California *Kepler* Survey (Petigura et al. 2017).

a few years have systematically higher metallicities than randomly chosen stars in the solar neighborhood (Gonzalez 1997; Santos et al. 2004; Fischer & Valenti 2005). In contrast, the host stars of smaller planets show little if any association with high metallicity (Udry et al. 2006; Sousa et al. 2011; Schlaufman & Laughlin 2011; Buchhave et al. 2012).[1] If all USP planets are the cores of former hot Jupiters, we should observe similar metallicity distributions for the hosts of USP planets and hot Jupiters. If instead the progenitors of USP planets are gaseous planets less massive than hot Jupiters, or if they form in the same way as somewhat longer-period planets, then the stars with USP planets should have a metallicity distribution similar to that of short-period sub-Neptunes. The metallicity distribution of *Kepler* planet hosts has been investigated previously by Buchhave et al. (2012); Mann et al. (2013); Buchhave et al. (2014); Dong et al. (2014); Schlaufman (2015); Buchhave & Latham (2015); Guo et al. (2016) and Mulders et al. (2016), but without special attention to USP planets. Our study focuses on USP planets, using the curated sample of Sanchis-Ojeda et al. (2014) and metallicities from new high-resolution spectroscopy by Petigura et al. (2017).

[1] We note, though, that these studies focused on stars near solar metallicity, and that Zhu et al. (2016) have questioned some of the evidence. Furthermore, Wang & Fischer (2015) found a metallicity effect for small planets, though not as strong as for giant planets; and Adibekyan et al. (2012) found that small-planet hosts tend to be higher in α-elements even if they are relatively poor in iron (the traditional metallicity indicator).

Section 2 describes our observations and sample selection. Section 3 compares the metallicity distributions of the host stars of hot Jupiters, sub-Neptunes, and USP planets. Section 5 compares our results to those of Mulders et al. (2016). Section 6 provides some concluding remarks.

2. OBSERVATIONS AND SAMPLE SELECTION

Sanchis-Ojeda et al. (2014; hereafter, SO+14) presented a catalog of USP planet candidates. We performed high-resolution optical spectroscopy of 71 of the stars in this sample with the Keck I telescope and HIRES (Vogt et al. 1994), as part of the larger California Kepler Survey (CKS; Petigura et al. 2017). All the stars brighter than $m_{\rm Kep} = 15.3$ were observed. Some fainter stars were also observed, particularly those hosting the planets with the shortest orbital periods. The spectra were collected from 2013 June to 2014 September. We used the standard California Planet Search setup, but without the iodine cell, giving a typical spectral resolution of $R = 60,000$ over the wavelength range 0.36-0.80 μm. The exposure times were typically 10 minutes, with a maximum exposure time of 20 minutes. For stars brighter than $m_{\rm Kep} = 14.3$, we achieved a signal-to-noise ratio (SNR) of 40 pixel^{-1} at 0.55 μm. For fainter stars, the SNR was between 20-40 pixel^{-1}.

The spectroscopic parameters of each star were determined with a combination of `SpecMatch`, a template-matching code; and a variant of *Spectroscopy Made Easy*, a spectral synthesis code. Details are provided by Petigura et al. (2017), who demonstrated a precision of 60 K in effective

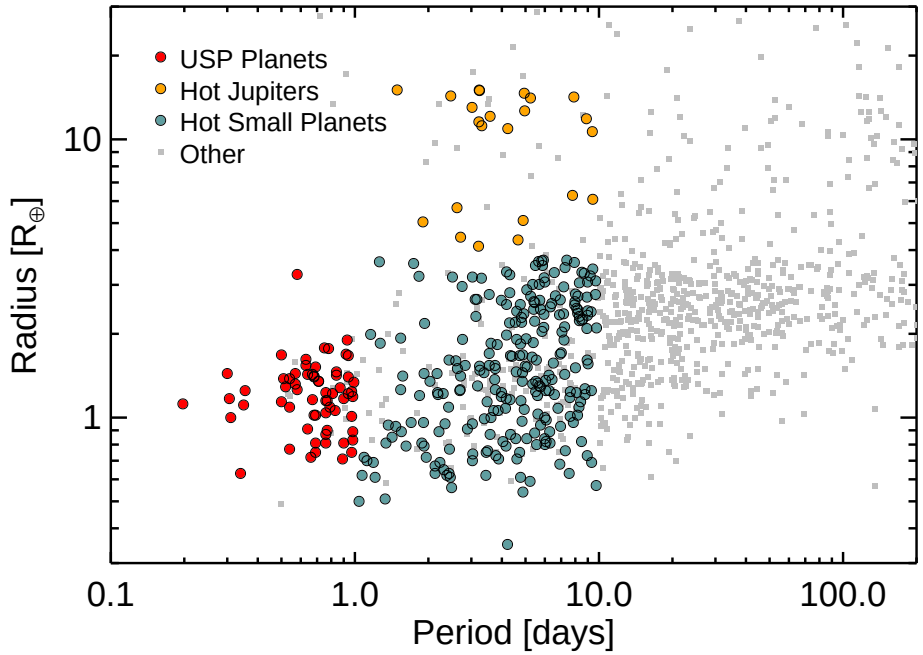


Figure 2. **Orbital period and planetary radius.** The colored circles show our statistical samples; the smaller squares are for the broader sample of stars in the California *Kepler* Survey (Petigura et al. 2017).

temperature, 0.07 dex in surface gravity, and 0.04 dex in [Fe/H].

For our study we omitted stars with $T_{\rm eff} < 4700$ K. There are severe discrepancies between the synthesized and observed spectra for such cool stars, due to the onset of molecular absorption that is poorly treated in the Coelho et al. (2005) models. We also removed KOI 2813 and KIC 5955905, for which the apparent transit signals have been shown to be caused by binary stars rather than transiting planets.[2]

The mass and radius of each star were determined by Johnson et al. (2017), based on the comparison of the observed spectroscopic parameters with those calculated with the Dartmouth Stellar Evolution Program (Dotter et al. 2008), using the `isochrones` code (Morton et al. 2016)[3]. The inputs were $T_{\rm eff}$, $\log g$, and [Fe/H], along with their associated uncertainties. The code produces *a posteriori* distributions for the stellar mass, radius, and age, by interpolating between the available Dartmouth models. The radii of the transiting planets were then calculated from the stellar radii and the measured transit depths.

3. METALLICITY DISTRIBUTIONS

We wanted to compare the metallicity distribution of the host stars of USP planets, hot Jupiters, and non-giant planets with periods longer than one day. To construct the appropriate samples we drew on the preceding results for the stars with USP planets, as well as the rest of the stars in the California *Kepler* Survey (Petigura et al. 2017). The larger sample includes about 1000 stars selected from the list of *Kepler* Objects of Interest (KOI), spanning a wide range of stellar types, planet sizes, and orbital periods. The stars were selected for spectroscopy independently of metallicity. Indeed, little information was available about the metallicities prior to the observations.

We restricted our attention to main-sequence stars with effective temperatures between 4700 and 6000 K, the range encompassing almost all of the stars with USP planets. We constructed three samples:

1. *USP Planets*: Stars having a planet with orbital period shorter than 1 day, selected from SO+14 as described above. This sample has 64 stars.

2. *Hot Jupiters*: Stars with a planet larger than 4 $R_\oplus$ and an orbital period shorter than 10 days. The somewhat arbitrary value of 4 $R_\oplus$ was chosen to match the value reported by Buchhave et al. (2012) and Buchhave et al. (2014) to distinguish different metallicity regimes. We omitted objects designated as "False Positives" by Twicken et al. (2016) or Santerne et al. (2016). We also omitted objects with inferred sizes larger than 20 $R_\oplus$ because experience has shown that in these

[2] KOI 2813 was identified as a probable spectroscopic binary by Kolbl et al. (2015). KIC 5955905 is a probable background binary, based on observations of large chromatic variations in the apparent transit depth (E. Palle, private communication).

[3] https://github.com/timothydmorton/isochrones (version 1.0)

cases the transit-like signal arises from a binary star rather than a transiting planet. This sample has 23 stars.

3. *Hot Small Planets*: Stars with planets smaller than 4 $R_\oplus$ and orbital periods between 1-10 days, after omitting objects designated as "False Positives". This sample has 246 stars.

Tables 1 and 2 give the pertinent properties of the USP Planets and Hot Jupiters. Figure 1 shows the spectroscopic parameters $T_{\rm eff}$ and $\log g$ for the stars in each sample. The dashed line is the boundary we used to identify main-sequence stars; our samples were restricted to stars below this line. Figure 2 shows the period-radius distribution of the planets hosted by the stars in each sample. In both figures, the small gray squares show the full sample of *Kepler* stars that were analyzed by Johnson et al. (2017).

Figure 3 focuses exclusively on the USP Planets. All but one of the USP planets have sizes $\lesssim 2\ R_\oplus$, even though no selection was made based on planet size. Thus, we confirm the finding of SO+14 that USP planets are almost always smaller than 2 $R_\oplus$. We find no major differences between our newly-determined radius distribution and the distribution presented by SO+14 except that the new estimates of planetary radii have smaller uncertainties, and one of the outliers with size $>2\ R_\oplus$ does not appear in the new sample. The single remaining USP planet with $R > 2\ R_\oplus$ is KOI 3913, a remarkable case which deserves further observations.

Figure 4 shows the distribution of [Fe/H] for the stars in each sample. Even at a glance, the Hot Jupiters are seen to be weighted toward higher [Fe/H] than either the USP Planets or the Hot Small Planets. The distributions for the USP and Hot Small Planets appear similar to one another. To quantify these impressions we performed two-sample Kolmogorov-Smirnov tests, which estimate the probability p that two samples are drawn from the same distribution. The results, given in Table 3, indicate that the USP Planets and Hot Jupiters are very unlikely to be drawn from the same distribution, while the USP Planets and the Hot Smaller Planets have distributions that are indistinguishable with the current data.

4. UPPER BOUND ON HOT-JUPITER FRACTION

Evidently the stars with USP planets have a different metallicity distribution than stars with hot Jupiters. We placed an upper bound on the fraction f of members in the USP Planet sample that could have been drawn from the same distribution as the Hot Jupiter sample, using a Monte Carlo technique. We considered the range of f from zero to unity. For each choice of f, we constructed a sample of 64 metallicities, matching the actual USP sample size. We randomly drew (with replacement) $N = [64f]$ values from the Hot Jupiter sample and $64-N$ values from the USP sample, where $[x]$ indicates rounding to the nearest integer. We added Gaussian errors to each metallicity with a standard deviation of 0.04 dex. We then computed the probability p that the simulated sample was drawn from the same underlying distribution as the Hot Jupiter sample, using a two-sided Kolmogorov-Smirnov test. We repeated this procedure 10^3 times and recorded the mean p value.

For high values of f, the simulated sample is drawn entirely from the USP Planets and the p-values are $\sim 10^{-3}$ as described in the previous section. For values of f approaching unity, the p-values are ~ 1 because the Hot Jupiter sample is being compared with itself. To determine an upper bound on f, we sought the value for which $p = 0.0455$, corresponding to a nominal 2σ level of confidence. The result is $f < 0.36$, implying that no more than about half of the metallicities of the USP host stars could have been drawn from the same metallicity distribution as the Hot Jupiter hosts.

5. COMPARISON WITH MULDERS ET AL. (2016)

Mulders et al. (2016) studied the relationship between orbital period and stellar metallicity for a sample of 665 *Kepler* planet candidates. They found the mean metallicity of stars with planets shorter than 10 days to be higher than for stars with longer-period planets. This was true for all planet sizes, with the strongest effect ($+0.25 \pm 0.07$ dex) seen for the smallest planets ($<1.7\ R_\oplus$).

Our study is concerned exclusively with planets with $P <$ 10 days. To compare our data with theirs, we note that their Fig. 2 shows the mean metallicity to be nearly constant for periods ranging from 0.6-5 days, before decreasing by $\approx$0.1 dex from 5-10 days. Our data does not display such a period dependence: the hosts of planets with periods $<$5 days and 5-10 days have the same mean metallicity to within 0.02 dex. A broader comparison between the CKS metallicity scale and that of Mulders et al. (2016) also shows significant differences, which will be examined as part of a forthcoming CKS paper led by E. Petigura.

We also note that our sample of ultra-short-period planets differs from that of Mulders et al. (2016). Our sample has 65 planets, while their sample has eight planets, three of which (KOI 2813, 2717 and 3204) have host stars with effective temperatures outside the range of our study (4700-6000 K).

6. CONCLUSIONS

The metallicity distribution of the host stars of USP planets does not resemble the metallicity distribution of the host stars of hot Jupiters. In particular, the stars with USP planets show no evidence for an association with high metallicity, unlike stars with hot Jupiters. The USP hosts have a mean metallicity near the Sun's value, and similar to that of the general planet-hosting population of *Kepler* stars.

This basic result is also obtained if we make some small changes to our sample definitions. If we require "Hot Jupiters" to have radii larger than 7 $R_\oplus$, instead of 4 $R_\oplus$, then the sample size decreases from 23 to 15. The metallicity dis-

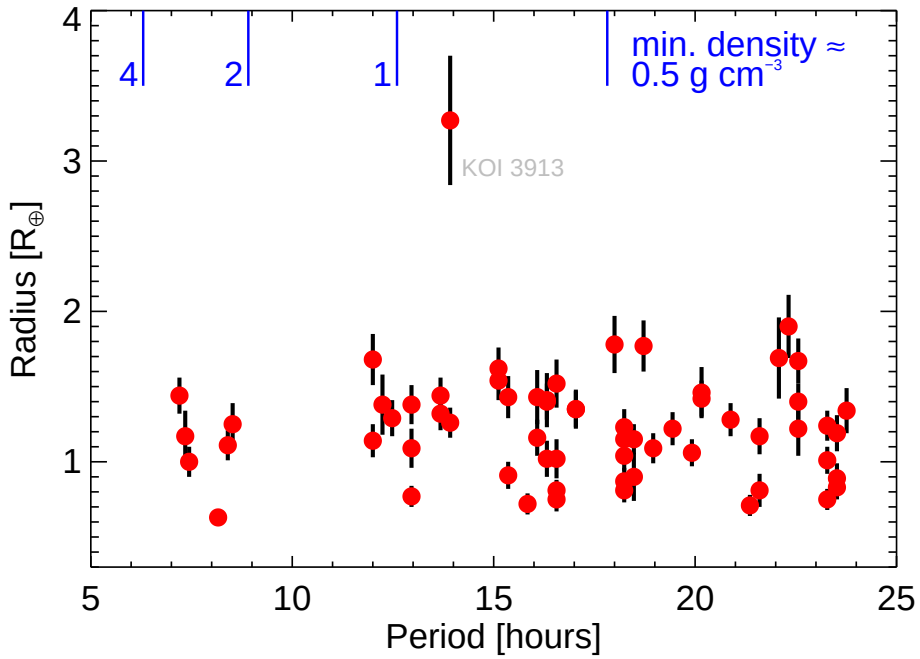


Figure 3. **Orbital period and planetary radius for USP planets.** Also marked are the Roche-limiting minimum periods for incompressible fluid bodies with mean densities of 0.5, 1.0, 2.0, and 4.0 g cm^{-3}, using Eqn. (2) of Rappaport et al. (2013). In reality, compression of the planetary interior may lower the minimum period by as much as ≈15%.

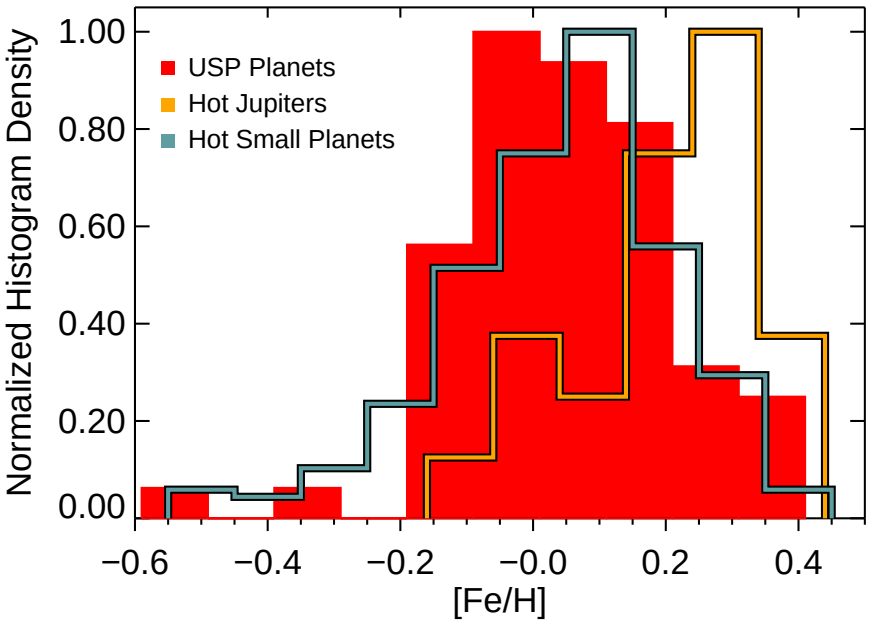


Figure 4. **Metallicity distributions** of the three statistical samples. The hot-Jupiter hosts have a different metallicity distribution (more weighted toward high metallicity) than the hosts of USP planets, and the hosts of planets smaller than Neptune with periods 1-10 days.

tribution of their host stars remains distinguishable from that of the stars with USP planets, though with reduced statistical significance ($p = 0.01$). We also tried requiring the "Hot Small Planets" to have radii between 2-4 $R_\oplus$, i.e., we omitted

the smaller planets that are more likely to be rocky. This is a more direct test of an evolutionary connection between USP planets and gas-rich planets at slightly longer periods. This reduces the sample size from 246 to 82. When tested against the metallicity distribution of the stars with USP planets, the p-value changes from 0.39 to 0.10, which is still too large to be considered evidence for a significant difference.

We interpret these results as an argument against any theory in which most of the USP planets are descended from hot Jupiters. In such a theory, the stars that are currently observed to have USP planets were once hosts to hot Jupiters, and their metallicity distribution should be the same as those stars currently observed to have hot Jupiters. The only way we see to escape this conclusion—which seems unlikely—is to hypothesize that the process that converts hot Jupiters into USP planets also systematically lowers the metallicity of the host star by $\Delta[\mathrm{Fe/H}] \approx -0.15$, so as to match the metallicity distribution of the hosts of smaller *Kepler* planets.

The possibility that USP planets represent the solid cores of erstwhile hot Jupiters had already been deemed unlikely on theoretical grounds, because of the difficulty of removing such a massive gaseous atmosphere. Murray-Clay et al. (2009) modeled the wind launched from a gaseous planet by a star's high-energy radiation, and found it difficult to erode the entire atmosphere of a hot Jupiter. Had we found a strong metallicity enhancement for the hosts of USP planets, this theoretical conclusion would have been called into question.

It remains plausible that the progenitors of USP planets are Neptune-sized or smaller planets with gaseous atmospheres. This is also compatible with the tendency of USP planets to have sub-Neptune companions in somewhat wider orbits (Sanchis-Ojeda et al. 2014; Adams et al. 2017). Multiple theoretical studies have shown that it is possible to lose most of the gas from a low-density planet smaller than Neptune (Howe & Burrows 2015; Lopez 2016; Jackson et al. 2017; Ginzburg & Sari 2016). Also consistent with this picture is the recent discovery by Fulton et al. (2017) that relatively few *Kepler* planets have sizes between 1.5-2 $R_\oplus$. The missing planets in this size range might have been gas-rich sub-Neptunes whose atmospheres were stripped.

Ultra-short-period planets remain an attractive subject for future work to understand their origin, occurrence rate, radius distribution, and the dependence of all these quantities on the properties of the host star. The current sample of $\sim$100 stars with USP planets have apparent magnitudes that are generally too faint for precise Doppler monitoring, observations of the Rossiter-McLaughlin effect, and detections of occultations or transmission effects. The *TESS* mission (Ricker et al. 2015) will help to remedy this problem by searching a similar number of stars as the *Kepler* mission, but brighter by several magnitudes.

We thank the anonymous referee for a prompt and helpful report. We thank Simon Albrecht, Eugene Chiang, Brian Jackson, Eve Lee, Peter McCullough, Saul Rappaport, Amaury Triaud and Francesca Valsecchi for helpful discussions. We also thank Enric Palle for sharing his results for KIC 5955905. J.N.W. acknowledges the support from a NASA Keck PI Data Award, administered by the NASA Exoplanet Science Institute. A.W.H. acknowledges the support from NASA grant NNX12AJ23G. Data presented herein were obtained at the W.M. Keck Observatory from telescope time allocated to the National Aeronautics and Space Administration through the agency's scientific partnership with the California Institute of Technology and the University of California. The Observatory was made possible by the generous financial support of the W.M. Keck Foundation. The authors acknowledge the very significant cultural role and reverence that the summit of Mauna Kea has always had within the indigenous Hawaiian community. We are most fortunate to have the opportunity to conduct observations from this mountain.

REFERENCES

Adams, E. R., Jackson, B., & Endl, M. 2016, AJ, 152, 47
Adams, E. R., Jackson, B., Endl, M., et al. 2017, AJ, 153, 82
Adibekyan, V. Z., Delgado Mena, E., Sousa, S. G., et al. 2012, A&A, 547, A36
Batalha, N. M., Borucki, W. J., Bryson, S. T., et al. 2011, ApJ, 729, 27
Becker, J. C., Vanderburg, A., Adams, F. C., Rappaport, S. A., & Schwengeler, H. M. 2015, ApJL, 812, L18
Buchhave, L. A., & Latham, D. W. 2015, ApJ, 808, 187
Buchhave, L. A., Latham, D. W., Johansen, A., et al. 2012, Nature, 486, 375
Buchhave, L. A., Bizzarro, M., Latham, D. W., et al. 2014, Nature, 509, 593
Chiang, E., & Laughlin, G. 2013, MNRAS, 431, 3444
Coelho, P., Barbuy, B., Meléndez, J., Schiavon, R. P., & Castilho, B. V. 2005, A&A, 443, 735
Dawson, R. I., & Fabrycky, D. C. 2010, ApJ, 722, 937
Demory, B.-O., Gillon, M., Deming, D., et al. 2011, A&A, 533, A114
Dong, S., Zheng, Z., Zhu, Z., et al. 2014, ApJL, 789, L3
Dotter, A., Chaboyer, B., Jevremović, D., et al. 2008, ApJS, 178, 89
Fischer, D. A., & Valenti, J. 2005, ApJ, 622, 1102
Fulton, B. J., Petigura, E. A., Howard, A. W., et al. 2017, ArXiv e-prints, arXiv:1703.10375 [astro-ph.EP]
Ginzburg, S., & Sari, R. 2016, ArXiv e-prints, arXiv:1611.09373 [astro-ph.EP]
Gonzalez, G. 1997, MNRAS, 285, 403
Guo, X., Johnson, J. A., Mann, A. W., et al. 2016, ArXiv e-prints, arXiv:1612.01616 [astro-ph.SR]
Howe, A. R., & Burrows, A. 2015, ApJ, 808, 150
Ida, S., & Lin, D. N. C. 2004, ApJ, 616, 567
Jackson, B., Arras, P., Penev, K., Peacock, S., & Marchant, P. 2017, ApJ, 835, 145
Jackson, B., Stark, C. C., Adams, E. R., Chambers, J., & Deming, D. 2013, ApJ, 779, 165
Johnson, J. A., Petigura, E. A., Fulton, B. J., et al. 2017, ArXiv e-prints, arXiv:1703.10402 [astro-ph.EP]
Kolbl, R., Marcy, G. W., Isaacson, H., & Howard, A. W. 2015, AJ, 149, 18
Lee, E. J., & Chiang, E. 2017, ArXiv e-prints, arXiv:1702.08461 [astro-ph.EP]

Léger, A., Rouan, D., Schneider, J., et al. 2009, A&A, 506, 287
Lopez, E. D. 2016, ArXiv e-prints, arXiv:1610.01170 [astro-ph.EP]
Lundkvist, M. S., Kjeldsen, H., Albrecht, S., et al. 2016, Nature Communications, 7, 11201
Mann, A. W., Gaidos, E., Kraus, A., & Hilton, E. J. 2013, ApJ, 770, 43
Morton, T. D., Bryson, S. T., Coughlin, J. L., et al. 2016, ApJ, 822, 86
Mulders, G. D., Pascucci, I., Apai, D., Frasca, A., & Molenda-Żakowicz, J. 2016, AJ, 152, 187
Murray-Clay, R. A., Chiang, E. I., & Murray, N. 2009, ApJ, 693, 23
Petigura, E. A., Howard, A. W., Marcy, G. W., et al. 2017, ArXiv e-prints, arXiv:1703.10400 [astro-ph.EP]
Rappaport, S., Sanchis-Ojeda, R., Rogers, L. A., Levine, A., & Winn, J. N. 2013, ApJL, 773, L15
Ricker, G. R., Winn, J. N., Vanderspek, R., et al. 2015, Journal of Astronomical Telescopes, Instruments, and Systems, 1, 014003
Rogers, L. A. 2015, ApJ, 801, 41
Sanchis-Ojeda, R., Rappaport, S., Winn, J. N., et al. 2014, ApJ, 787, 47
—. 2013, ApJ, 774, 54
Santerne, A., Moutou, C., Tsantaki, M., et al. 2016, A&A, 587, A64
Santos, N. C., Israelian, G., & Mayor, M. 2004, A&A, 415, 1153
Schlaufman, K. C. 2015, ApJL, 799, L26
Schlaufman, K. C., & Laughlin, G. 2011, ApJ, 738, 177
Schlaufman, K. C., Lin, D. N. C., & Ida, S. 2010, ApJL, 724, L53
Sousa, S. G., Santos, N. C., Israelian, G., Mayor, M., & Udry, S. 2011, A&A, 533, A141
Steffen, J. H., & Coughlin, J. L. 2016, Proceedings of the National Academy of Science, 113, 12023
Terquem, C. 2014, MNRAS, 444, 1738
Twicken, J. D., Jenkins, J. M., Seader, S. E., et al. 2016, AJ, 152, 158
Udry, S., Mayor, M., Benz, W., et al. 2006, A&A, 447, 361
Valsecchi, F., Rasio, F. A., & Steffen, J. H. 2014, ApJL, 793, L3
Vanderburg, A., Bieryla, A., Duev, D. A., et al. 2016, ApJL, 829, L9
Vogt, S. S., Allen, S. L., Bigelow, B. C., et al. 1994, in Proc. SPIE, Vol. 2198, Instrumentation in Astronomy VIII, ed. D. L. Crawford & E. R 362
Wang, J., & Fischer, D. A. 2015, AJ, 149, 14
Weiss, L. M., & Marcy, G. W. 2014, ApJL, 783, L6
Winn, J. N., Matthews, J. M., Dawson, R. I., et al. 2011, ApJL, 737, L18
Zhu, W., Wang, J., & Huang, C. 2016, ApJ, 832, 196

Table 1. Characteristics of "USP Planet" sample

ID	$T_{\rm eff}$ [K]	$\log g$	[Fe/H]	$R_\star$ [$R_\odot$]	$M_\star$ [$M_\odot$]	R_p [$R_\oplus$]	$P_{\rm orb}$ [hr]
KOI 0072	5599^{+66}_{-65}	$4.340^{+0.080}_{-0.100}$	$-0.110^{+0.040}_{-0.040}$	$1.060^{+0.160}_{-0.090}$	$0.910^{+0.040}_{-0.030}$	$1.46^{+0.17}_{-0.17}$	20.2
KOI 0191	5459^{+63}_{-64}	$4.450^{+0.070}_{-0.080}$	$0.100^{+0.040}_{-0.040}$	$0.940^{+0.090}_{-0.060}$	$0.920^{+0.030}_{-0.030}$	$1.35^{+0.12}_{-0.12}$	17.0
KOI 0577	5085^{+64}_{-66}	$4.530^{+0.040}_{-0.040}$	$0.110^{+0.040}_{-0.040}$	$0.820^{+0.040}_{-0.040}$	$0.830^{+0.030}_{-0.030}$	$0.91^{+0.09}_{-0.09}$	15.4
KOI 0717	5619^{+61}_{-68}	$4.250^{+0.090}_{-0.100}$	$0.310^{+0.040}_{-0.040}$	$1.280^{+0.170}_{-0.140}$	$1.050^{+0.060}_{-0.040}$	$0.81^{+0.11}_{-0.11}$	21.6
KOI 1128	5352^{+65}_{-63}	$4.500^{+0.060}_{-0.060}$	$-0.040^{+0.040}_{-0.040}$	$0.870^{+0.060}_{-0.050}$	$0.860^{+0.030}_{-0.030}$	$1.24^{+0.10}_{-0.10}$	23.3
KOI 1150	5755^{+68}_{-66}	$4.320^{+0.090}_{-0.090}$	$0.100^{+0.040}_{-0.040}$	$1.150^{+0.140}_{-0.110}$	$1.010^{+0.040}_{-0.040}$	$1.02^{+0.12}_{-0.12}$	16.3
KOI 1169	5634^{+66}_{-64}	$4.360^{+0.090}_{-0.090}$	$0.110^{+0.040}_{-0.040}$	$1.080^{+0.130}_{-0.100}$	$0.970^{+0.030}_{-0.030}$	$1.52^{+0.16}_{-0.16}$	16.6
KOI 1239	5747^{+66}_{-66}	$4.380^{+0.070}_{-0.080}$	$-0.040^{+0.040}_{-0.040}$	$1.050^{+0.110}_{-0.080}$	$0.970^{+0.040}_{-0.030}$	$1.77^{+0.17}_{-0.17}$	18.7
KOI 1300	4764^{+63}_{-65}	$4.580^{+0.030}_{-0.030}$	$0.030^{+0.040}_{-0.040}$	$0.740^{+0.020}_{-0.020}$	$0.760^{+0.030}_{-0.020}$	$1.54^{+0.13}_{-0.13}$	15.1
KOI 1360	4960^{+64}_{-64}	$4.590^{+0.030}_{-0.040}$	$-0.100^{+0.040}_{-0.040}$	$0.740^{+0.030}_{-0.020}$	$0.780^{+0.030}_{-0.030}$	$0.87^{+0.09}_{-0.09}$	18.2
KOI 1367	4962^{+64}_{-64}	$4.590^{+0.030}_{-0.040}$	$-0.080^{+0.040}_{-0.040}$	$0.750^{+0.030}_{-0.020}$	$0.780^{+0.030}_{-0.030}$	$1.44^{+0.12}_{-0.12}$	13.7
KOI 1428	4776^{+64}_{-65}	$4.600^{+0.030}_{-0.030}$	$-0.110^{+0.040}_{-0.040}$	$0.710^{+0.030}_{-0.020}$	$0.730^{+0.030}_{-0.030}$	$1.90^{+0.21}_{-0.21}$	22.3
KOI 1442	5568^{+58}_{-70}	$4.260^{+0.090}_{-0.100}$	$0.390^{+0.040}_{-0.040}$	$1.260^{+0.160}_{-0.140}$	$1.050^{+0.060}_{-0.040}$	$1.43^{+0.18}_{-0.18}$	16.1
KOI 1655	5536^{+64}_{-65}	$4.450^{+0.070}_{-0.070}$	$-0.070^{+0.040}_{-0.040}$	$0.940^{+0.080}_{-0.060}$	$0.900^{+0.030}_{-0.030}$	$1.40^{+0.12}_{-0.12}$	22.6
KOI 1688	5979^{+71}_{-64}	$4.100^{+0.100}_{-0.100}$	$0.170^{+0.040}_{-0.040}$	$1.620^{+0.290}_{-0.210}$	$1.220^{+0.120}_{-0.080}$	$1.69^{+0.27}_{-0.27}$	22.1
KOI 1875	5576^{+65}_{-64}	$4.400^{+0.070}_{-0.080}$	$-0.110^{+0.040}_{-0.040}$	$0.980^{+0.100}_{-0.080}$	$0.900^{+0.030}_{-0.030}$	$1.38^{+0.13}_{-0.13}$	13.0
KOI 2039	5575^{+64}_{-64}	$4.490^{+0.030}_{-0.060}$	$0.250^{+0.040}_{-0.040}$	$0.950^{+0.060}_{-0.040}$	$1.010^{+0.030}_{-0.040}$	$0.81^{+0.08}_{-0.08}$	18.2
KOI 2079	5477^{+68}_{-66}	$4.380^{+0.080}_{-0.090}$	$0.380^{+0.040}_{-0.040}$	$1.070^{+0.120}_{-0.090}$	$1.000^{+0.040}_{-0.030}$	$0.75^{+0.08}_{-0.08}$	16.6
KOI 2093	5953^{+66}_{-65}	$4.350^{+0.070}_{-0.080}$	$0.020^{+0.040}_{-0.040}$	$1.140^{+0.130}_{-0.100}$	$1.070^{+0.040}_{-0.040}$	$1.34^{+0.15}_{-0.15}$	23.8
KOI 2119	5136^{+65}_{-65}	$4.540^{+0.040}_{-0.050}$	$0.180^{+0.040}_{-0.040}$	$0.830^{+0.040}_{-0.030}$	$0.870^{+0.030}_{-0.030}$	$1.32^{+0.11}_{-0.11}$	13.7
KOI 2202	5307^{+64}_{-65}	$4.470^{+0.060}_{-0.070}$	$0.320^{+0.040}_{-0.040}$	$0.930^{+0.080}_{-0.050}$	$0.940^{+0.030}_{-0.030}$	$1.22^{+0.11}_{-0.11}$	19.4
KOI 2248	5149^{+65}_{-64}	$4.540^{+0.040}_{-0.050}$	$0.110^{+0.040}_{-0.040}$	$0.830^{+0.040}_{-0.030}$	$0.850^{+0.030}_{-0.030}$	$1.15^{+0.10}_{-0.10}$	18.2
KOI 2250	4958^{+65}_{-66}	$4.570^{+0.030}_{-0.040}$	$0.120^{+0.040}_{-0.040}$	$0.780^{+0.030}_{-0.030}$	$0.820^{+0.030}_{-0.030}$	$1.62^{+0.14}_{-0.14}$	15.1
KOI 2281	5080^{+65}_{-65}	$4.530^{+0.040}_{-0.040}$	$0.160^{+0.040}_{-0.040}$	$0.820^{+0.040}_{-0.040}$	$0.840^{+0.030}_{-0.030}$	$0.90^{+0.16}_{-0.16}$	18.5
KOI 2393	4836^{+65}_{-65}	$4.590^{+0.030}_{-0.040}$	$-0.060^{+0.040}_{-0.040}$	$0.730^{+0.030}_{-0.020}$	$0.760^{+0.030}_{-0.030}$	$1.15^{+0.10}_{-0.10}$	18.5
KOI 2396	5228^{+66}_{-65}	$4.540^{+0.040}_{-0.060}$	$0.100^{+0.040}_{-0.040}$	$0.830^{+0.050}_{-0.030}$	$0.870^{+0.030}_{-0.030}$	$1.68^{+0.17}_{-0.17}$	12.0
KOI 2409	4774^{+65}_{-66}	$4.660^{+0.030}_{-0.020}$	$-0.590^{+0.040}_{-0.040}$	$0.620^{+0.020}_{-0.020}$	$0.630^{+0.020}_{-0.020}$	$1.26^{+0.10}_{-0.10}$	13.9
KOI 2492	5635^{+62}_{-60}	$4.370^{+0.080}_{-0.090}$	$-0.310^{+0.040}_{-0.040}$	$0.980^{+0.110}_{-0.090}$	$0.830^{+0.030}_{-0.030}$	$0.89^{+0.10}_{-0.10}$	23.5
KOI 2517	5601^{+64}_{-64}	$4.520^{+0.030}_{-0.060}$	$-0.070^{+0.040}_{-0.040}$	$0.880^{+0.050}_{-0.040}$	$0.940^{+0.030}_{-0.030}$	$1.01^{+0.09}_{-0.09}$	23.3
KOI 2571	5269^{+65}_{-66}	$4.480^{+0.060}_{-0.070}$	$0.250^{+0.040}_{-0.040}$	$0.900^{+0.070}_{-0.050}$	$0.910^{+0.040}_{-0.030}$	$1.06^{+0.09}_{-0.09}$	19.9
KOI 2607	5774^{+63}_{-65}	$4.400^{+0.070}_{-0.090}$	$0.200^{+0.040}_{-0.040}$	$1.070^{+0.120}_{-0.080}$	$1.050^{+0.040}_{-0.040}$	$1.78^{+0.19}_{-0.19}$	18.0
KOI 2668	5460^{+66}_{-66}	$4.510^{+0.050}_{-0.060}$	$-0.040^{+0.040}_{-0.040}$	$0.870^{+0.060}_{-0.040}$	$0.900^{+0.030}_{-0.030}$	$1.40^{+0.12}_{-0.12}$	16.3
KOI 2694	4787^{+65}_{-66}	$4.560^{+0.030}_{-0.030}$	$0.230^{+0.040}_{-0.040}$	$0.770^{+0.030}_{-0.030}$	$0.790^{+0.030}_{-0.030}$	$1.42^{+0.12}_{-0.12}$	20.2
KOI 2753	5840^{+55}_{-63}	$4.170^{+0.100}_{-0.100}$	$0.210^{+0.040}_{-0.040}$	$1.450^{+0.230}_{-0.190}$	$1.130^{+0.100}_{-0.060}$	$1.22^{+0.18}_{-0.18}$	22.6

Table 1 continued

Table 1 *(continued)*

ID	$T_{\rm eff}$ [K]	$\log g$	[Fe/H]	$R_\star$ [$R_\odot$]	$M_\star$ [$M_\odot$]	R_p [$R_\oplus$]	$P_{\rm orb}$ [hr]
KOI 2756	5904^{+66}_{-61}	$4.380^{+0.070}_{-0.090}$	$0.100^{+0.040}_{-0.040}$	$1.100^{+0.130}_{-0.090}$	$1.070^{+0.040}_{-0.040}$	$1.16^{+-0.12}_{--0.12}$	16.1
KOI 2763	4727^{+65}_{-65}	$4.600^{+0.030}_{-0.030}$	$-0.010^{+0.040}_{-0.040}$	$0.720^{+0.020}_{-0.020}$	$0.750^{+0.030}_{-0.030}$	$1.14^{+-0.11}_{--0.11}$	12.0
KOI 2796	5686^{+68}_{-65}	$4.350^{+0.080}_{-0.100}$	$0.000^{+0.040}_{-0.040}$	$1.080^{+0.140}_{-0.100}$	$0.960^{+0.030}_{-0.030}$	$1.09^{+-0.13}_{--0.13}$	13.0
KOI 2874	5243^{+64}_{-65}	$4.510^{+0.060}_{-0.050}$	$-0.080^{+0.040}_{-0.040}$	$0.840^{+0.050}_{-0.050}$	$0.820^{+0.030}_{-0.030}$	$1.11^{+-0.10}_{--0.10}$	8.4
KOI 2875	4967^{+63}_{-64}	$4.580^{+0.030}_{-0.040}$	$-0.090^{+0.040}_{-0.040}$	$0.750^{+0.030}_{-0.030}$	$0.770^{+0.030}_{-0.030}$	$1.44^{+-0.12}_{--0.12}$	7.2
KOI 2879	5472^{+65}_{-66}	$4.510^{+0.040}_{-0.060}$	$-0.010^{+0.040}_{-0.040}$	$0.880^{+0.060}_{-0.040}$	$0.910^{+0.030}_{-0.030}$	$0.63^{+-0.05}_{--0.05}$	8.2
KOI 2916	4978^{+65}_{-65}	$4.560^{+0.040}_{-0.040}$	$-0.000^{+0.040}_{-0.040}$	$0.770^{+0.030}_{-0.030}$	$0.800^{+0.030}_{-0.030}$	$1.00^{+-0.10}_{--0.10}$	7.4
KOI 3009	5110^{+65}_{-64}	$4.550^{+0.040}_{-0.050}$	$0.170^{+0.040}_{-0.040}$	$0.820^{+0.040}_{-0.030}$	$0.860^{+0.030}_{-0.030}$	$1.04^{+-0.10}_{--0.10}$	18.2
KOI 3032	5213^{+64}_{-65}	$4.430^{+0.060}_{-0.060}$	$0.360^{+0.040}_{-0.040}$	$0.950^{+0.080}_{-0.060}$	$0.900^{+0.030}_{-0.030}$	$1.43^{+-0.14}_{--0.14}$	15.4
KOI 3065	5713^{+63}_{-64}	$4.480^{+0.040}_{-0.070}$	$-0.000^{+0.040}_{-0.040}$	$0.940^{+0.070}_{-0.050}$	$0.980^{+0.030}_{-0.030}$	$1.17^{+-0.12}_{--0.12}$	21.6
KOI 3246	4847^{+66}_{-66}	$4.580^{+0.030}_{-0.040}$	$0.130^{+0.040}_{-0.040}$	$0.760^{+0.030}_{-0.020}$	$0.800^{+0.030}_{-0.030}$	$0.81^{+-0.07}_{--0.07}$	16.6
KOI 3867	5566^{+67}_{-63}	$4.420^{+0.070}_{-0.090}$	$0.140^{+0.040}_{-0.040}$	$0.990^{+0.100}_{-0.070}$	$0.960^{+0.030}_{-0.030}$	$1.67^{+-0.15}_{--0.15}$	22.6
KOI 3913	5952^{+65}_{-63}	$4.260^{+0.090}_{-0.100}$	$0.180^{+0.040}_{-0.040}$	$1.310^{+0.190}_{-0.150}$	$1.140^{+0.060}_{-0.050}$	$3.27^{+-0.43}_{--0.43}$	13.9
KOI 4002	5207^{+64}_{-64}	$4.530^{+0.040}_{-0.060}$	$0.200^{+0.040}_{-0.040}$	$0.850^{+0.050}_{-0.040}$	$0.890^{+0.030}_{-0.030}$	$1.29^{+-0.12}_{--0.12}$	12.5
KOI 4018	5479^{+64}_{-65}	$4.520^{+0.040}_{-0.060}$	$-0.010^{+0.040}_{-0.040}$	$0.870^{+0.050}_{-0.040}$	$0.920^{+0.030}_{-0.030}$	$1.28^{+-0.11}_{--0.11}$	20.9
KOI 4070	4926^{+66}_{-65}	$4.570^{+0.030}_{-0.040}$	$0.070^{+0.040}_{-0.040}$	$0.770^{+0.030}_{-0.030}$	$0.800^{+0.030}_{-0.030}$	$1.09^{+-0.10}_{--0.10}$	19.0
KOI 4072	5840^{+61}_{-65}	$4.260^{+0.100}_{-0.100}$	$0.110^{+0.040}_{-0.040}$	$1.270^{+0.170}_{-0.140}$	$1.060^{+0.050}_{-0.040}$	$1.02^{+-0.13}_{--0.13}$	16.6
KOI 4109	4995^{+66}_{-66}	$4.530^{+0.040}_{-0.040}$	$0.250^{+0.040}_{-0.040}$	$0.830^{+0.040}_{-0.040}$	$0.840^{+0.030}_{-0.030}$	$0.72^{+-0.07}_{--0.07}$	15.8
KOI 4144	6000^{+65}_{-64}	$4.390^{+0.070}_{-0.080}$	$-0.110^{+0.040}_{-0.040}$	$1.080^{+0.110}_{-0.080}$	$1.030^{+0.040}_{-0.040}$	$1.19^{+-0.12}_{--0.12}$	23.5
KOI 4159	5233^{+66}_{-66}	$4.490^{+0.060}_{-0.050}$	$0.120^{+0.040}_{-0.040}$	$0.880^{+0.050}_{-0.050}$	$0.860^{+0.030}_{-0.030}$	$0.75^{+-0.07}_{--0.07}$	23.3
KOI 4199	5109^{+65}_{-65}	$4.570^{+0.030}_{-0.050}$	$-0.120^{+0.040}_{-0.040}$	$0.770^{+0.040}_{-0.030}$	$0.800^{+0.030}_{-0.030}$	$0.77^{+-0.07}_{--0.07}$	13.0
KOI 4366	5269^{+66}_{-63}	$4.530^{+0.050}_{-0.060}$	$-0.110^{+0.040}_{-0.040}$	$0.820^{+0.050}_{-0.040}$	$0.830^{+0.030}_{-0.030}$	$1.23^{+-0.12}_{--0.12}$	18.2
KOI 4430	5104^{+65}_{-66}	$4.550^{+0.040}_{-0.050}$	$0.100^{+0.040}_{-0.040}$	$0.810^{+0.040}_{-0.030}$	$0.840^{+0.030}_{-0.030}$	$1.38^{+-0.20}_{--0.20}$	12.2
KOI 4441	4888^{+65}_{-65}	$4.570^{+0.030}_{-0.030}$	$0.060^{+0.040}_{-0.040}$	$0.760^{+0.030}_{-0.030}$	$0.790^{+0.030}_{-0.030}$	$1.41^{+-0.18}_{--0.18}$	16.3
KOI 4469	4909^{+65}_{-64}	$4.570^{+0.030}_{-0.040}$	$0.070^{+0.040}_{-0.040}$	$0.770^{+0.030}_{-0.030}$	$0.800^{+0.030}_{-0.030}$	$0.71^{+-0.07}_{--0.07}$	21.4
KOI 4746	4948^{+66}_{-66}	$4.570^{+0.030}_{-0.040}$	$0.080^{+0.040}_{-0.040}$	$0.780^{+0.030}_{-0.030}$	$0.810^{+0.030}_{-0.030}$	$0.83^{+-0.08}_{--0.08}$	23.5
KOI 4841	4803^{+65}_{-65}	$4.590^{+0.030}_{-0.030}$	$-0.010^{+0.040}_{-0.040}$	$0.730^{+0.030}_{-0.020}$	$0.760^{+0.030}_{-0.030}$	$1.35^{+-0.13}_{--0.13}$	17.0
KIC 8435766	5060^{+65}_{-64}	$4.570^{+0.030}_{-0.040}$	$0.000^{+0.040}_{-0.040}$	$0.780^{+0.030}_{-0.030}$	$0.820^{+0.030}_{-0.030}$	$1.25^{+0.14}_{-0.14}$	8.5
KIC 11187332	5573^{+66}_{-65}	$4.430^{+0.070}_{-0.070}$	$-0.090^{+0.040}_{-0.040}$	$0.960^{+0.090}_{-0.070}$	$0.900^{+0.030}_{-0.030}$	$1.17^{+0.17}_{-0.17}$	7.3
KIC 2718885	5614^{+64}_{-64}	$4.370^{+0.080}_{-0.090}$	$0.120^{+0.040}_{-0.040}$	$1.060^{+0.120}_{-0.090}$	$0.960^{+0.030}_{-0.030}$	$1.12^{+0.19}_{-0.19}$	4.7

Table 2. Characteristics of "Hot Jupiter" sample

ID	$T_{\rm eff}$ [K]	$\log g$	[Fe/H]	$R_\star$ [$R_\odot$]	$M_\star$ [$M_\odot$]	R_p [$R_\oplus$]	$P_{\rm orb}$ [hr]
KOI 0001	5815^{+66}_{-65}	$4.390^{+0.080}_{-0.090}$	$0.010^{+0.040}_{-0.040}$	$1.060^{+0.120}_{-0.090}$	$1.010^{+0.030}_{-0.030}$	$14.32^{+-1.42}_{--1.42}$	59.3
KOI 0003	4867^{+66}_{-65}	$4.540^{+0.040}_{-0.030}$	$0.310^{+0.040}_{-0.040}$	$0.810^{+0.030}_{-0.030}$	$0.830^{+0.030}_{-0.030}$	$5.11^{+-0.41}_{--0.41}$	117.4
KOI 0007	5833^{+60}_{-67}	$4.120^{+0.110}_{-0.100}$	$0.170^{+0.040}_{-0.040}$	$1.530^{+0.240}_{-0.200}$	$1.120^{+0.100}_{-0.060}$	$4.13^{+-0.60}_{--0.60}$	77.0
KOI 0017	5667^{+58}_{-63}	$4.170^{+0.100}_{-0.100}$	$0.340^{+0.040}_{-0.040}$	$1.450^{+0.220}_{-0.180}$	$1.110^{+0.100}_{-0.060}$	$15.04^{+-2.10}_{--2.10}$	77.5
KOI 0022	5885^{+61}_{-58}	$4.210^{+0.100}_{-0.100}$	$0.200^{+0.040}_{-0.040}$	$1.380^{+0.210}_{-0.180}$	$1.130^{+0.090}_{-0.060}$	$14.20^{+-2.02}_{--2.02}$	189.4
KOI 0063	5660^{+64}_{-63}	$4.490^{+0.030}_{-0.050}$	$0.230^{+0.040}_{-0.040}$	$0.960^{+0.050}_{-0.040}$	$1.030^{+0.030}_{-0.030}$	$6.09^{+-0.49}_{--0.49}$	226.3
KOI 0127	5600^{+58}_{-67}	$4.350^{+0.080}_{-0.090}$	$0.350^{+0.040}_{-0.040}$	$1.130^{+0.140}_{-0.100}$	$1.040^{+0.040}_{-0.040}$	$12.10^{+-1.29}_{--1.29}$	85.9
KOI 0128	5669^{+66}_{-67}	$4.210^{+0.090}_{-0.100}$	$0.250^{+0.040}_{-0.040}$	$1.330^{+0.210}_{-0.150}$	$1.050^{+0.070}_{-0.050}$	$14.65^{+-1.99}_{--1.99}$	118.6
KOI 0135	5951^{+68}_{-66}	$4.210^{+0.100}_{-0.120}$	$0.320^{+0.040}_{-0.040}$	$1.450^{+0.260}_{-0.190}$	$1.230^{+0.090}_{-0.060}$	$13.03^{+-2.05}_{--2.05}$	72.5
KOI 0141	5322^{+65}_{-63}	$4.430^{+0.070}_{-0.070}$	$0.300^{+0.040}_{-0.040}$	$0.970^{+0.090}_{-0.070}$	$0.930^{+0.030}_{-0.030}$	$5.68^{+-0.53}_{--0.53}$	62.9
KOI 0186	5802^{+62}_{-63}	$4.350^{+0.080}_{-0.090}$	$0.180^{+0.040}_{-0.040}$	$1.130^{+0.140}_{-0.100}$	$1.050^{+0.040}_{-0.040}$	$14.97^{+-1.60}_{--1.60}$	77.8
KOI 0195	5535^{+64}_{-66}	$4.480^{+0.060}_{-0.070}$	$-0.160^{+0.040}_{-0.040}$	$0.890^{+0.080}_{-0.060}$	$0.870^{+0.030}_{-0.030}$	$11.56^{+-0.93}_{--0.93}$	77.3
KOI 0201	5526^{+69}_{-67}	$4.240^{+0.100}_{-0.100}$	$0.350^{+0.040}_{-0.040}$	$1.260^{+0.170}_{-0.140}$	$1.020^{+0.050}_{-0.040}$	$10.93^{+-1.35}_{--1.35}$	101.5
KOI 0203	5714^{+64}_{-64}	$4.440^{+0.040}_{-0.070}$	$0.310^{+0.040}_{-0.040}$	$1.030^{+0.080}_{-0.050}$	$1.080^{+0.030}_{-0.040}$	$15.05^{+-1.20}_{--1.20}$	35.8
KOI 0214	5481^{+72}_{-66}	$4.310^{+0.090}_{-0.090}$	$0.390^{+0.040}_{-0.040}$	$1.160^{+0.140}_{-0.120}$	$1.000^{+0.040}_{-0.040}$	$11.19^{+-1.27}_{--1.27}$	79.4

Table 2 continued

Table 2 *(continued)*

ID	$T_{\rm eff}$ [K]	$\log g$	[Fe/H]	$R_\star$ [$R_\odot$]	$M_\star$ [$M_\odot$]	R_p [$R_\oplus$]	$P_{\rm orb}$ [hr]
KOI 0439	5458^{+65}_{-65}	$4.370^{+0.080}_{-0.090}$	$0.320^{+0.040}_{-0.040}$	$1.070^{+0.120}_{-0.090}$	$0.980^{+0.030}_{-0.030}$	$5.05^{+-0.51}_{-0.51}$	45.6
KOI 0466	5954^{+66}_{-63}	$4.210^{+0.100}_{-0.100}$	$0.040^{+0.040}_{-0.040}$	$1.360^{+0.190}_{-0.160}$	$1.090^{+0.050}_{-0.040}$	$10.66^{+-1.79}_{-1.79}$	225.4
KOI 0760	5741^{+66}_{-65}	$4.360^{+0.080}_{-0.090}$	$0.090^{+0.040}_{-0.040}$	$1.090^{+0.130}_{-0.100}$	$1.000^{+0.040}_{-0.030}$	$12.66^{+-1.31}_{-1.31}$	119.0
KOI 0800	5904^{+63}_{-61}	$4.250^{+0.100}_{-0.100}$	$0.200^{+0.040}_{-0.040}$	$1.310^{+0.200}_{-0.150}$	$1.130^{+0.070}_{-0.050}$	$4.45^{+-0.63}_{-0.63}$	65.0
KOI 0889	5311^{+63}_{-66}	$4.480^{+0.060}_{-0.070}$	$0.220^{+0.040}_{-0.040}$	$0.910^{+0.070}_{-0.050}$	$0.900^{+0.040}_{-0.030}$	$11.86^{+-0.95}_{-0.95}$	213.1
KOI 1779	5861^{+63}_{-65}	$4.420^{+0.040}_{-0.060}$	$0.300^{+0.040}_{-0.040}$	$1.080^{+0.080}_{-0.060}$	$1.130^{+0.040}_{-0.040}$	$4.35^{+-0.35}_{-0.35}$	111.8
KOI 1800	5611^{+65}_{-65}	$4.510^{+0.030}_{-0.050}$	$0.070^{+0.040}_{-0.040}$	$0.910^{+0.050}_{-0.030}$	$0.980^{+0.030}_{-0.030}$	$6.29^{+-0.55}_{-0.55}$	187.0
KOI 3689	5988^{+68}_{-67}	$4.190^{+0.100}_{-0.110}$	$0.030^{+0.040}_{-0.040}$	$1.410^{+0.220}_{-0.170}$	$1.110^{+0.060}_{-0.040}$	$14.08^{+-1.98}_{-1.98}$	125.8

Table 3. Comparisons between metallicity distributions

Sample name	Number of stars	Sample mean [Fe/H]	p for comparison[a] with USPs	p for comparison[a] with Hot Jupiters
USP Planets	64	0.0584 ± 0.0050	⋯	3×10^{-4}
Hot Jupiters	23	0.2096 ± 0.0085	3×10^{-4}	⋯
Hot Small Planets	246	0.0459 ± 0.0026	0.39	2×10^{-5}

[a] Probability of being drawn from the same distribution, based on a two-sample Kolmogorov-Smirnov test.